Journal of Organometallic Chemistry 889 (2019) 62–69

Contents lists available at ScienceDirect

Journal of Organometallic Chemistry

journal homepage: www.elsevier.com/locate/jorganchem

Synthesis and characterization of acrylate cyanide bridged dimeric fac-Rhenium(I) complex: Photophysical, selective CO_2 adsorption and theoretical studies

Debopam Sinha, Sankar Prasad Parua**, Kajal Krishna Rajak*

Inorganic Chemistry Section, Department of Chemistry, Jadavpur University, Kolkata, 700032, India

ARTICLE INFO

Article history:
Received 6 August 2018
Received in revised form
14 March 2019
Accepted 15 March 2019
Available online 21 March 2019

Keywords:
Cyclic binuclear Re(I) complex
X-ray structure
Photoluminescence
Selective CO_2 adsorption
Computational studies

ABSTRACT

Reaction of ethyl 2-cyano-3-(2-hydroxy-5-methyl-3-(p-tolylimino)methyl)phenyl)acrylate) (HL) based on 2, 6-diformyl-4-methylphenol with $[Re(CO)_5Cl]$ in toluene afforded a product of composition $[Re_2(CO)_6(L)_2]$. X-ray structure of the representative complex $[Re_2(CO)_6(L)_2]$ was determined to confirm the molecular species unequivocally. The molecular structure of the rhenium complex exhibited distorted octahedral geometry around the Re(I) center, consistent with the d^6 configuration. The complex exhibited excellent photoluminescence behavior in acetonitrile solution. To gain a deeper insight into the ground and excited-state geometries, absorption, and emission properties of the binuclear Re(I) core, complex was further scrutinized by DFT and TDDFT methods. In addition, the synthesized binuclear Re(I) complex was used as a porous material for the selective adsorption of CO_2 gas at low temperature (273 K), as well as at ambient condition (298 K). To the best of our knowledge, this compound is the first Re(I)-based binuclear complex which efficiently adsorbs CO_2 selectively.

1. Introduction

The research on the field of photophysical and photochemical properties of the coordination complexes of transition metals has received an increasing interest since the last few decades due to their potential application in chemical biology and materials chemistry [1–5]. In connection with this different transition metal complexes of heavier metal ions, especially those with d^6 electronic configuration, such as rhenium(I) [6], ruthenium(II) [7], osmium(II) [8], rhodium(III) [9] and iridium(III) [10] were studied by various spectroscopic as well as by the electrochemical techniques. In comparison to the other transition metal complexes with d^6, MLCT system, rhenium(I) complexes of general formula *fac*-$[Re(CO)_3]^+$ were found to show intense luminescence and its origin has been attributed to the triplet metal Re(I) to ligand charge transfer(^{3}MLCT) excited state and/or intra ligand charge-transfer (ILCT) states [11,12].

The Re(I) complexes has wide applications due to their unique characteristics of chemical stability, strong visible absorption, excited state reactivity and catalytic properties. The behavior of such types complexes has received increasing interest to exploit these materials for solar energy conversion, organic light-emitting devices, electron transfer reaction, reduction of CO_2 in a homogeneous solution as well as at the electrode surfaces and in the field of bioimaging [13–23]. Moreover, the photophysical properties of the metal complex can widely be tuned by modification of both the metal center and the ligand structure [24].

In this context the main challenge is to design and synthesis of the chromophoric ligands with suitably donor sites which induce the formation of the stable metal complex with a concomitant increase in their r.t. luminescence lifetime [25]. Pyridine and its derivatives are among the most widely used ligands due to their efficient coordination to transition metals [26] but there are no reports on the studies of rhenium(I) complexes having the *fac*-$[Re(CO)_3]^+$ moiety with bidentate N,O donor Schiff base ligands bearing ethylcyano-vinyl fragment.

Herein, we have reported the synthesis of a hitherto unknown phenyl acrylate cyanide bridged binuclear Re(I) complex using the bidentate (N,O donor) Schiff base ligand, HL [27].

The complex formation has been authenticated on the basis of single crystal X-ray studies and 1HNMR spectroscopy. The

* Corresponding author.
** Corresponding author.
E-mail addresses: sankubengal@gmail.com (S.P. Parua), kajalrajak@gmail.com (K.K. Rajak).

https://doi.org/10.1016/j.jorganchem.2019.03.014
0022-328X/

photophysical behavior of the newly synthesized complex has also been described. Moreover we have investigated the application of a binuclear Re(I) complex as an adsorbent for the selective adsorption of CO_2 at low temperature as well as room temperature. To get a better insight into the geometry and the electronic structure, geometry optimization of the ground and excited states and spectral properties of these complex, density functional theory (DFT) and time dependent density functional theory (TD-DFT) studies have also been included.

2. Results and discussion

2.1. Synthesis

The reaction of HL ligand with the commercially available precursor $[Re(CO)_5Cl]$ in 1:1 stoichiometric ratios in dry toluene under refluxing condition afforded solid complex of the composition $[Re_2(CO)_6(L)_2]$ in excellent yield (Scheme 1). Its structure was confirmed by X-ray crystallography.

2.2. Characterization

The ligand HL and complex $[Re_2(CO)_6(L)_2]$ was characterized satisfactorily by IR, ^1H NMR and ^{13}C NMR spectroscopy (Fig. S1-S4). The IR spectra of $[Re_2(CO)_6(L)_2]$ exhibited the characteristic νC≡N, νC = N, and νC = O(-COOEt) absorption near 2219 cm^{-1}, 1585 cm^{-1}, and 1708 cm^{-1} respectively. The facial νCO observed at 2014 cm^{-1} and 1901 cm^{-1} respectively. For the complex νC≡N (2219 cm^{-1}) slightly shifted to lower frequency than the νC≡N (2222 cm^{-1}) of the free ligand [27] indicating the coordination of cyanide nitrogen.

The ^1H NMR spectra of the complex $[Re_2(CO)_6(L)_2]$ was recorded in DMSO-d6(Fig. S3). The Phenolic OH signal of HL (δ 14.61) ligand(S2) [27] were absent in the spectra of the complex signifying the coordination of phenoxide O. Azomethine (-N=CH-) proton(H_a) resonance of $[Re_2(CO)_6(L)_2]$ complex is observed as a singlet at δ 8.88 ppm. In the complex H_c and H_d are observed as singlet at 8.26 and 7.65 ppm. H_e and H_f are observed as doublet at 7.28 and 7.21 ppm in the complex $[Re_2(CO)_6(L)_2]$ respectively. Two aromatic methyl group of $[Re_2(CO)_6(L)_2]$ complex appeared at δ 2.36 ppm and δ 2.24 ppm respectively. The methylene(-CH_2) and methyl(-CH_3) proton resonance of ethyl group of ester moiety appeared as quadrate at δ 4.30 ppm and triplet at δ 1.31 ppm respectively. The ^1H NMR spectral features for the aromatic protons of the ligand HL and complex $[Re_2(CO)_6(L)_2]$ matched well with the composition and structure. Relevant ^1H NMR spectral data of the complex is collected in experimental section.

2.3. Crystal structure description

Single crystals suitable for structure determination were isolated by slow diffusion of hexane into dichloromethane solution of $[Re_2(CO)_6(L)_2]$. The crystallographic data collection and refinement parameters are given in Table S1; selected bond distances and angles are given in Table S2. A perspective view with the atom numbering scheme is shown in Fig. 1.

Single-crystal X-ray crystallographic study revealed that the discrete binuclear $[Re_2(CO)_6(L)_2]$ complex crystallizes in a triclinic system with space group P-1. The molecular structure of binuclear $[Re_2(CO)_6(L)_2]$ complex exhibits a distorted octahedral geometry around each rhenium, where the anionic ligand L^- binds the metal through phenolato oxygen, imine nitrogen and cyanide nitrogen. Three carbonyl ligand completes the hexa-coordination about Re(I). The binuclear Re(I) core is surrounded by two HL ligands and six carbonyl groups (Fig. S5.). Overall, the complex $[Re_2(CO)_6(L)_2]$ exhibits 2D framework (Fig. 2a).

The layers are stabilized by π ⋯ π (4.23 A^0) interactions among the para cresol rings of HL and O⋯CH (2.83 A^0) interaction between oxygen of ethoxy group and methyl hydrogen of the para cresol ring of the ligand (Fig. 2b).

The phase purity of bulk sample of $[Re_2(CO)_6(L)_2]$ complex was confirmed by the powder X-ray diffraction studies. The experimental PXRD patterns are well matched with the simulated results, indicating the phase purity of the rhenium complex (Fig. S6).

2.4. Geometry optimization, electronic structure

To get an insight into the ground state geometry, electronic structure of the binuclear Re(I) complex $[Re_2(CO)_6(L)_2]$, geometry optimization was performed in solution phase assuming a singlet ground state (S = 0, t_2g^6). The geometry utilized for the ground state optimization is based on crystal structure parameter of the complex $[Re_2(CO)_6(L)_2]$ with ligand modification. The optimized bond distances and bond angles of the complex $[Re_2(CO)_6(L)_2]$ are given in Table S3.

The optimized geometrical structure of the $[Re_2(CO)_6(L)_2]$ complex at singlet ground (S_0) state is shown in Fig. S7. As depicted in Fig. S7 each Re(I) center of $[Re_2(CO)_6(L)_2]$ complex displays the distorted octahedral geometry with a facial arrangement of three CO ligands at each center. The optimized parameters of the complex $[Re_2(CO)_6(L)_2]$ matched well with the X-ray crystal structure data. These results clearly represent that there are no significant changes of the ligand framework in the binuclear Re(I) complex. The isodensity plot from H-5 to L+5 for $[Re_2(CO)_6(L)_2]$ is shown in Fig. 3.

The energy and compositions of selected frontier molecular orbital of the $[Re_2(CO)_6(L)_2]$ complex in singlet ground state (S_0) are listed in Table 1.

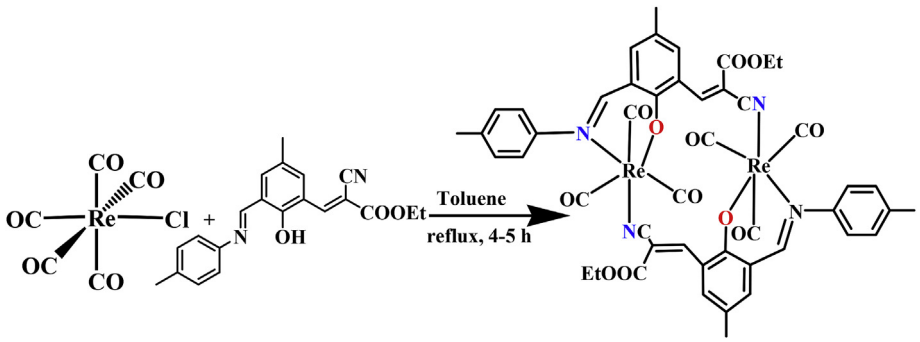

Scheme 1. Schematic representation for the synthesis of the $[Re_2(CO)_6(L)_2]$ complex.

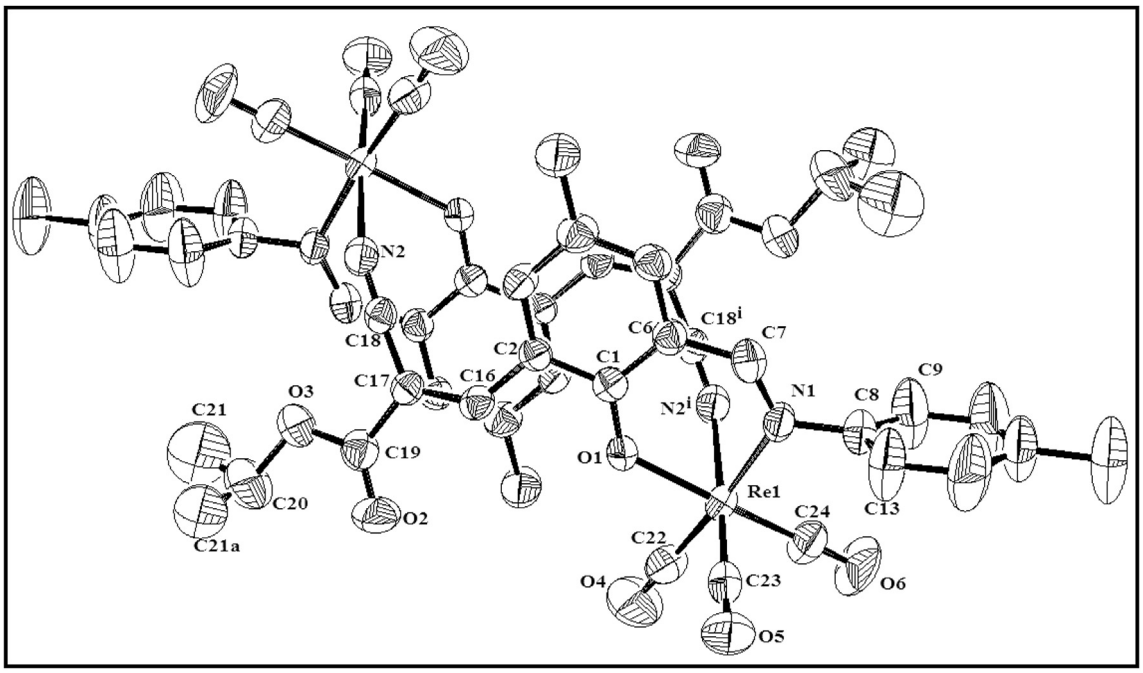

Fig. 1. ORTEP and atom-numbering scheme for $[Re_2(CO)_6(L)_2]$ complex. Hydrogen atoms are omitted for clarity.

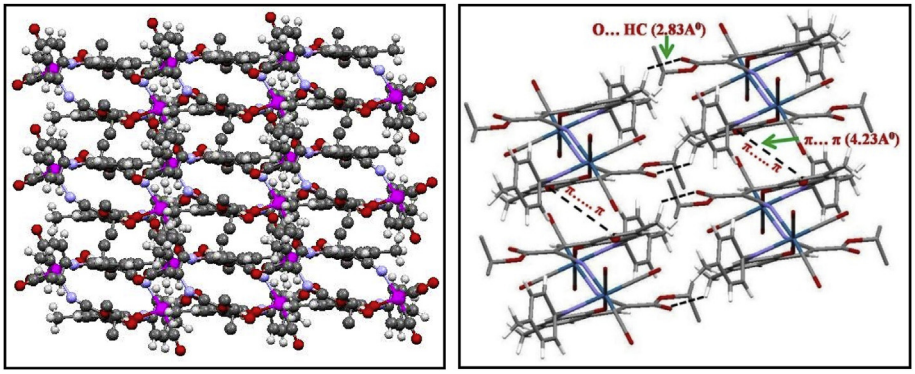

Fig. 2. (a) Perspective view of the 2D framework (b) Illustration of CH···O and π···π interactions stabilizing the 2D framework.

2.5. Excited state (T_1)

The DFT calculation have also been performed for geometry optimization of the binuclear Re(I) complex in their low lying excited triplet (T_1) state in solution phase. The optimized geometrical structure of the rhenium complex in low lying excited triplet state is given in the Supplementary materials (Fig. S8) and the geometrical parameters are given in Table S3. Most interestingly, the geometry around both the rhenium centre's in S_0 and T_1 states remain almost same although significant changes have been occur in the ligand frame which corroborated that ligand bind in a similar fashion in the complex. The calculated C=N (imine) bond distance at T_1 state occurs ~1.18 Å in the complex $[Re_2(CO)_6(L)_2]$ which is similar with the ground state (Table S3). The isodensity surfaces of HSOMO, LSOMO and electronic spin density for complex $[Re_2(CO)_6(L)_2]$ at the relaxed T_1 geometry are shown in Fig. 4.

The electron density in HSOMO of $[Re_2(CO)_6(L)_2]$ complex is mainly due to the major contribution of *p*-cresol moiety and π orbital of ethyl cyano acryl fragment of the ligand(Fig. 4) and resembles with the corresponding LUMO and L+1 of the S_0 geometry. On the other hand the electron density of LSOMO mainly resides on the metal centre along with small contribution of the π orbital of acrylate bond(C=C) of the ligand. The spin density plot of the complex at the triplet state (T_1) demonstrates that the electron density mainly localized on ligand moiety with small contribution of metal orbital. Thus the low lying triplet excited state (T_1) in the complex $[Re_2(CO)_6(L)_2]$ is mainly intraligand (^{3}IL) excited [28].

2.6. TDDFT calculation and electronic spectra

The electronic spectra of both the ligand HL and complex $[Re_2(CO)_6(L)_2]$ were recorded in acetonitrile solution at room temperature. The ligand HL displayed moderate intense peak at 370 nm and very low intense peak at 500 nm. The $[Re_2(CO)_6(L)_2]$ complex exhibited moderately intense peak at 475 nm and high intense peak at 300 nm (Fig. 5).

In order to elucidate the electronic transitions from a theoretical perspective, TDDFT/B3LYP/CPCM calculation on the optimized geometry of the complex $[Re_2(CO)_6(L)_2]$ has been performed in acetonitrile. In the TDDFT calculation we found highly intense

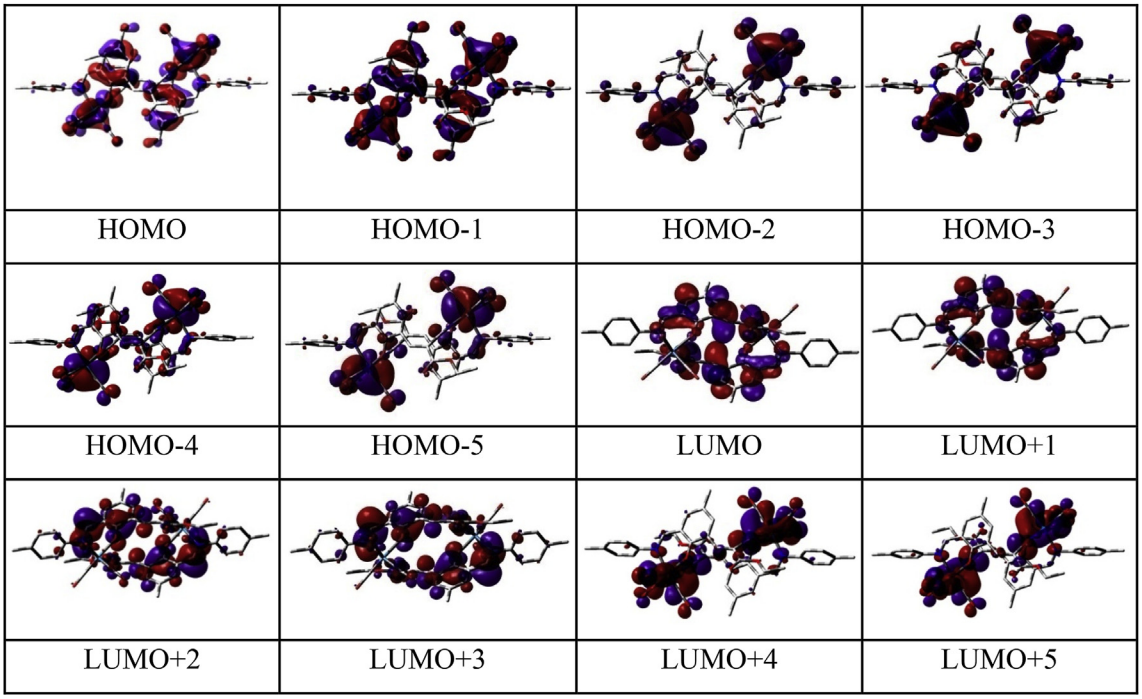

Fig. 3. Isodensity plot of frontier orbitals of $[Re_2(CO)_6(L)_2]$ complex.

Table 1
Energy and composition of selected molecular orbitals of $[Re_2(CO)_6(L)_2]$.

MO	Energy (eV)	% of composition						Main bond types
		Re	CO	Ligand				
				imi	p-tol	p-cres	acryl	
LUMO+5	−1.27	23	52	0	2	0	12	p(Re) +л*(acryl) +л*(CO)
LUMO+4	−1.31	26	48	0	2	1	10	p(Re) +л*(acryl) +л*(CO)
LUMO+3	−2.27	2	6	22	2	13	8	л*(imi) +л*(p-cres) + л*(acryl)
LUMO+2	−2.29	1	7	24	1	14	7	л*(imi) +л*(p-cres)
LUMO+1	−3.02	1	2	2	0	17	29	л*(p-cres) + л*(acryl)
LUMO	−3.06	1	0	3	0	18	28	л*(p-cres) + л*(acryl)
HOMO	−5.79	24	15	1	2	24	4	d(Re)+л(p-cres)+л(CO)
HOMO-1	−5.96	22	12	2	2	26	3	d(Re)+л(CO) +л(p-cres)
HOMO-2	−6.46	57	26	0	4	4	1	d(Re)+л(CO)
HOMO-3	−6.49	53	24	1	2	8	1	d(Re)+л(CO)+л(p-cres)
HOMO-4	−6.58	57	24	0	2	5	3	d(Re)+л(CO)
HOMO-5	−6.63	61	25	2	1	3	2	d(Re)+л(CO)

The value of the energy difference between HOMO and LUMO of the complex $[Re_2(CO)_6(L)_2]$ equals to 2.73 eV. The highest occupied orbital (HOMO) and H-1 are mainly consisted of л orbital of p-cresol to the rhenium d orbital with some contribution of л orbital of CO molecule. In the complex $[Re_2(CO)_6(L)_2]$, H-2 is predominantly localized on the rhenium centre with significant contribution of the л orbital of CO molecule. The energy of HOMO-3 and HOMO-4 are almost same (energy difference ~ 0.09 eV in the complex $[Re_2(CO)_6(L)_2]$. The electron density of the LUMO (L) and L+1 of complex $[Re_2(CO)_6(L)_2]$, originates from p-cresol and acrylate л* orbital localized on C=C bond and aromatic system.

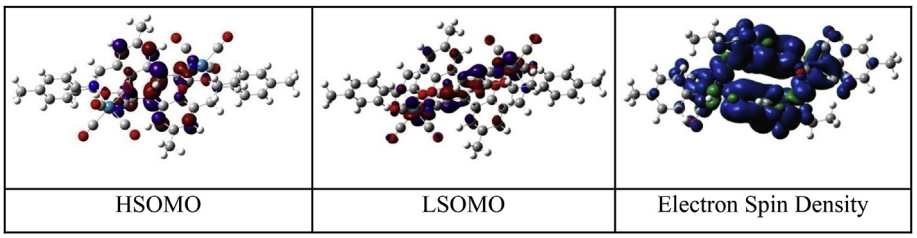

Fig. 4. Isodensity surface plots of HSOMO, LSOMO and electron spin density for the complex $[Re_2(CO)_6(L)_2]$ at T_1 state geometry. Blue and green colors regions represent the positive and negative difference between the alpha and beta electron densities, respectively. (For interpretation of the references to color in this figure legend, the reader is referred to the Web version of this article.)

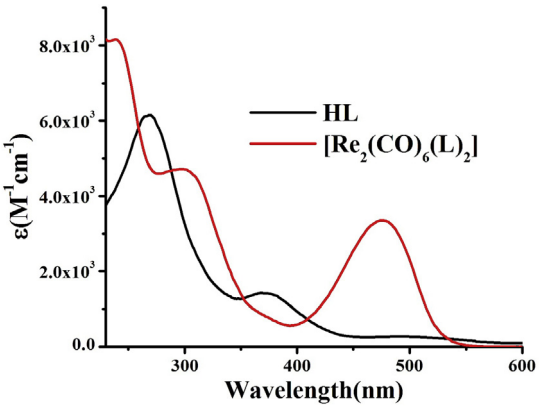

Fig. 5. UV–vis spectra of HL and $[Re_2(CO)_6(L)_2]$ complex.

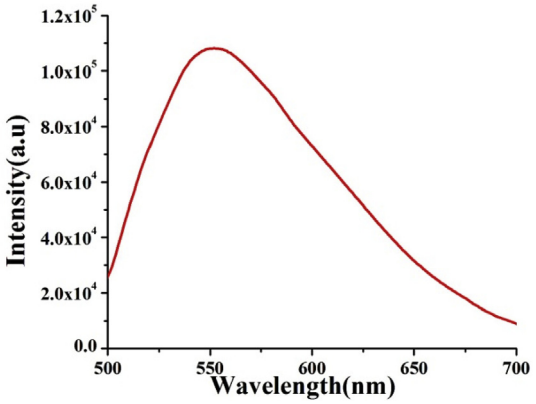

Fig. 6. Emission spectra of complex in acetonitrile solution, at room temperature ($\lambda_{ex} = 480$ nm, $\lambda_{em} = 550$ nm).

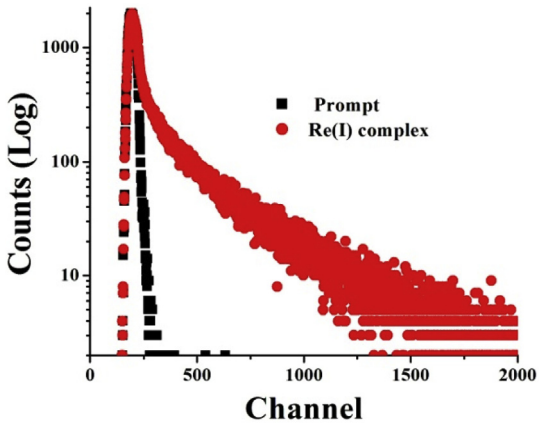

Fig. 7. Time-resolved fluorescence lifetime decay of $[Re_2(CO)_6(L)_2]$ complex.

transition at 502 nm (f = 0.2765) corresponds to H-1→ LUMO having ^{1}MLCT character with little ^{1}ILCT (Table 2) [29].

The highest energy band with maxima at 309 nm for complex $[Re_2(CO)_6(L)_2]$ can rationally be assigned to an admixture of metal-to-ligand charge transfer (^{1}MLCT) transition and spin-allowed π→ π*(ligand-centered, ^{1}ILCT) transitions [29].

2.7. Emission spectral properties

To investigate the emission property of the binuclear rhenium(I) complex, photoluminescence measurement in solution state was performed.

The complex $[Re_2(CO)_6(L)_2]$ exhibited strong photo-luminescence near 595 nm on excitation at 480 nm (quantum yield (Φ) ca.0.04) (Fig. 6). The emission intensity of Re(I) complex can be attributed to the triplet metal Re(I) to ligand charge transfer(^{3}MLCT) excited state [28].

Furthermore the time resolved luminescence spectra also give evidence to understand the decay process and the emissive nature of the complex. Life time data are recorded for complex $[Re_2(CO)_6(L)_2]$ at room temperature in acetonitrile solution when excited at 480 nm. The observed luminescence decay fit with bi-exponential decay nature of the complex $[Re_2(CO)_6(L)_2]$ (Fig. 7).

The fluorescence life time (t), radiative (k_r) and nonradiative (k_{nr}) decay rate constant of the complex $[Re_2(CO)_6(L)_2]$ are collected in Table 3.

To simulate the experimental luminescence spectra, unrestricted B3LYP method for the Re(I) complex in triplet(T_1) state has been performed in acetonitrile. The main reason behind the emission spectra of the compound is the excited triplet(T_1) state charge transfer transitions and electronic spin density(Fig. 4) which indicating the ligand centered ^{3}IL nature of the complex. The calculated emission energy associated with their oscillator strength, the main configurations and their assignments as well as the experimental result of $[Re_2(CO)_6(L)_2]$ are listed in (Table 4). TD-DFT study at T_1 state for the complex $[Re_2(CO)_6(L)_2]$ substantiates with the ^{3}ILCT nature for the complex $[Re_2(CO)_6(L)_2]$ transitions.[29].

Table 2
Main calculated optical transition for the complex $[Re_2(CO)_6(L)_2]$ with composition in terms of molecular orbital contribution of the transition, vertical excitation energies, and oscillator strength in acetonitrile.

Composition	Excitation Energy(eV)	Osc.Strength (f)	Assign	CI	λ_{exp} (nm)
H-1→ L	2.46(502 nm)	0.2765	^{1}MLCT/^{1}ILCT	0.68	475
H-1→ L+4	4.00(309 nm)	0.0110	^{1}MLCT/^{1}ILCT	0.52	300
H→ L+5			^{1}ILCT		

2.8. Gas sorption study

The vacant space in the cyclic binuclear Re(I) complex was confirmed by the crystallographic structure, encouraged us to investigate the porosity of the complex. In this regard gas sorption study of the complex was performed and verified the selectivity in adsorption amongst the small molecule gasses like N_2, H_2, and CO_2. Interestingly, the $[Re_2(CO)_6(L)_2]$ complex showed the selective adsorption of CO_2 gas at low and room temperature. The synthesized binuclear rhenium complex was directly used as an active material for the sorption experiment because of the absence of guest molecule in the crystal lattice. The CO_2 gas sorption isotherm at low temperature (273 K) and room temperature (298 K) was almost same and shows a typical type III nature with a maximum value of 5.07 wt% or 25.70 mL/g gas [30] uptakes at low pressure respectively, suggesting the porous nature of the complex (Fig. 8). The BET (Brunauer-Emmett-Teller) surface area estimated from the CO_2 sorption isotherms is 18.6 m^2/g. The hydrogen uptake of $[Re_2(CO)_6(L)_2]$ complex reached about 0.20 wt% or 22.8 mL/g at the adsorbate pressure of 1 bar at 77 K (Fig. 8).On the other hand, the complex did not show any significant uptake of N_2 at 77 K. To get profound insight, we have calculated isosteric heats of adsorption (Q_{st}) of CO_2 applying Clausius-Clapeyron equation at two different temperatures viz. 273 K and 298 K [31]. Q_{st} (-ΔH, adsorption

Table 3
The photophysical parameters of the complex $[Re_2(CO)_6(L)_2]$ in acetonitrile solution at room temperature.

Sample	τ_1, ns	τ_2, ns	τ_{av}	$\Phi(\times10^{-3})$	$k_r/s^{-1}(x10^5)$ (±5%error)	$k_{nr}/s^{-1}(\times10^7)$ (±5%error)
$[Re_2(CO)_6(L)_2]$	1.8(43%)	7.2(57%)	2.98	3.62	5.04	13.89

Table 4
Calculated triplet excited state of $[Re_2(CO)_6(L)_2]$ in acetonitrile solution based on the lowest lying triplet state geometry. Main calculated vertical transitions with compositions in terms of molecular orbital contribution of the transition, vertical excitation energies and oscillator strength.

Excitation	Composition	Excitation Energy	Oscillator Strength (f)	Assign	λ_{exp}(nm)
1	H-13(β)→L(β) H-12(β)→L+1(β)	2.229eV (556 nm)	0.002	^{3}ILCT ^{3}ILCT	550

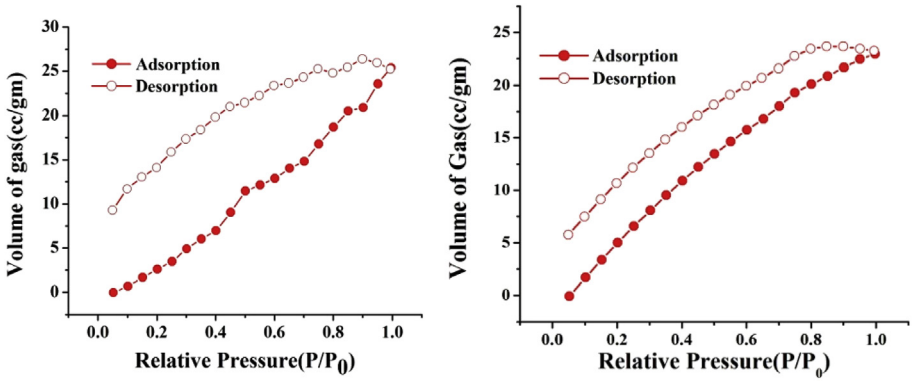

Fig. 8. (a) CO_2 sorption isotherm at 298 K (b) H_2 sorption isotherm at 77 K.

enthalpy) value for complex $[Re_2(CO)_6(L)_2]$ is about 11.2 kJ/mol (Fig. S9).

Most interesting fact is that the structural integrity of the recovered sample remained almost similar after CO_2 gas adsorption (Fig. S6).

3. Conclusions

In summary, the cyclic binuclear Re(I) complex could be prepared upon reaction of the ligand HL, with appropriate metal substrate. The structure of the $[Re_2(CO)_6(L)_2]$ complex was confirmed by X-Ray crystallography studies. The photophysical properties of Re(I) complex have been investigated. As application, the new binuclear $[Re_2(CO)_6(L)_2]$ complex have been used as porous material for the adsorption studies of the small molecule gasses like N_2, H_2, and CO_2. More importantly, the complex exhibited highly selective uptake (5.07 wt%) of CO_2 gas at low temperature as well as room temperature. To the best of our knowledge this is the first report on the use of binuclear Re(I) complex as porous material for the selective adsorption of CO_2 gas. The present work investigated the ground and excited-state geometries, absorption, and luminescence properties of $[Re_2(CO)_6(L)_2]$ complex by DFT and TDDFT methods.

4. Experimental section

4.1. Materials and methods

$[Re(CO)_5Cl]$ (98%) used was purchased from Aldrich Chemical Co. The ligand Ethyl2-cyano-3-(2-hydroxy-5-methyl-3-(p-tolylimino)methyl)phenyl)acrylate, (HL) was prepared following the reported procedure [27]. All the chemicals and solvents were analytically pure and used without further purification. Infrared spectra were recorded on a Perkin-Elmer L120-00A FT-IR spectrometer with the samples prepared as KBr pellets. ^{1}H NMR spectra was recorded on a Bruker FT 400 MHz instrument. For NMR spectra, $CDCl_3$ and DMSO-d6 was used as the solvent using TMS as an internal standard. UV–vis experiments were performed on a Perkin–Elmer LAMBDA 25 spectrophotometer and the fluorescence experiment was performed using Horiba Fluoromax-4 fluorescence spectrometer and a fluorescence cell of 10 mm path length. Elemental analysis (C, H, and N) was performed on a Perkin-Elmer 2400 series II analyzer. Quantum yield of the complex $[Re_2(CO)_6(L)_2]$ was determined in freeze-pump-thaw-degassed solution of the complex by a relative method using quinine sulphate as the standard [$\Phi_{std} = 0.54$ (at 298 K) in 0.1 M H_2SO_4 at $\lambda_{ex} = 350$ nm] [32]. Time-correlated single photon counting (TCSPC) measurement was carried out for the luminescence decay of complex $[Re_2(CO)_6(L)_2]$ in acetonitrile. For TCSPC measurement, the photoexcitation was made at 480 nm using a picoseconds diode laser (IBH Nanoled-07) in an IBH Fluorocube apparatus. The fluorescence decay data were collected on a Hamamatsu MCP photomultiplier (R3809) and were analyzed by using IBH DAS6 software. Gas sorption isotherms were measured in the pressure range of 0–1 bar using an Autosorb iQ (Quantachorme Inc., USA) gas sorption system. For all isotherms, warm and cold free space correction measurements were performed using ultrahigh purity helium gas (99.999% purity). N_2 and H_2 isotherms at 77 K were measured in a liquid nitrogen bath using UHP-grade gas sources.

4.2. Computational details

The geometrical structure of the singlet ground state (S_0) and the lowest lying triplet excited state (T_1) were optimized using the

density functional theory (DFT) [33] method at the RB3LYP and UB3LYP levels of theory [34]. The geometry of the binuclear Re(I) complex was fully optimized in solution phase with imposing centre of symmetry constraint. The absorption spectral properties of the binuclear Re(I) complex based on the optimized ground state geometry structure was computed using the time dependent density functional theory (TDDFT) [35] approach in acetonitrile associated with the conductor-like polarizable continuum model (CPCM) [36]. In the calculation, the quasirelativistic pseudopotentials of Re atoms proposed by Hay and Wadt [37] with 14 valence electrons (outer-core [(5s^{2}5p6)] electrons and the (5 d^6) valence electrons) were employed, and a "double-ξ" quality basis set LANL2DZ was adopted as the basis set for Re atoms. The 6-31G basis set was used for the C, H, N and O atoms for the optimization of both the ground state and the lowest lying triplet excited state geometries. All the calculations were performed using the Gaussian 09W software package [38]. The GaussSum 2.1 program [39] was used to calculate the molecular orbital contributions from groups or atoms.

4.3. Crystallographic studies

Single Crystals of $[Re_2(CO)_6(L)_2]$ complex was grown by slow diffusion of hexane in dichloromethane solution at 25 °C. Data were collected on a Bruker SMART CCD diffractometer using Mo-Kα monochromator (λ = 0.71073). Structure solutions were performed using Shelx 97 PC version program [40]. Full matrix least square refinements on F2 were performed using SHELXL-97 program [41]. All the non-hydrogen atoms were refined anisotropically using full-matrix least squares method. Hydrogen atoms were included for structure factor calculations after placing them at calculated positions. The ethyl group (-Et) of ethyl ester fragment (-COOEt) for $[Re_2(CO)_6(L)_2]$ complex was found to be disordered that could not be refined satisfactorily but that did not cause much difficulty toward unequivocal characterization of the complex. Atomic coordinates and isotropic thermal parameters of $[Re_2(CO)_6(L)_2]$ are given in Table S1.

4.4. Synthesis

4.4.1. Synthesis of $[Re_2(CO)_6(L)_2]$ complex

To a stirred solution of HL (70 mg, 0.20 mmol) in 20 mL of dry toluene, $[Re(CO)_5Cl]$ (73 mg, 0.20 mmol) and triethylamine (0.028 mL, 0.20 mmol) were added and then the resulting mixture was refluxed for 4–5 h under argon atmosphere. After cooling to room temperature, the solvent was removed under reduced pressure. The crude product was dissolved in dichloromethane and was purified by thin layer chromatography on silica plate with toluene/CH_3CN (95:5) as the eluent. A pink brown band separated and the complex was extracted from silica with dichloromethane and methanol. The pink brown solid, obtained upon evaporation of the solvent, was recrystallized from dichloromethane-hexane. Yield: 105 mg (74%). Elemental Anal. Calcd for $C_{48}H_{44}N_4O_{12}Re_2$: C, 46.44; H, 3.57; N, 4.51. Found: C, 46.52; H, 3.45; N, 4.46. IR (KBr pellets, cm^{-1}): ν(Facial 3CO) 2014, 1901 and 1708; ν(C=N) 1617, νC≡N(2220) (νC = O) 1708. ^{1}H NMR DMSO-d6: δ (ppm), J (Hz): 8.88 (s, 1H), 8.48 (s, 1H), 8.26 (s, 1H), 7.65 (s, 1H) 7.28 (d, 2H, J = 8), 7.14 (d, 2H, J = 8.0), 4.30 (q, 2H, J = 8), 2.36 (s, 3H), 2.24 (s, 3H), 1.31 (t, 3H, J = 4). ^{13}C NMR DMSO-d6: δ (ppm) 196.7, 165.6, 162.0, 161.8, 152.9, 148.5, 142.7, 135.0, 133.9, 128.2, 128.1, 127.9, 122.5, 121.4, 121.3, 121.0, 115.3, 96.9, 61.02, 60.9, 29.6, 19.4, 18.7, 12.9.

Acknowledgments

D.S. thanks The RUSA 2.0 for research fellowship.

S.P.P. thanks the DST-SERB (New Delhi) for research fellowship. The necessary laboratory and infrastructural facility are provided by the Department of Chemistry, Jadavpur University.

Appendix A. Supplementary data

Supplementary data to this article can be found online at https://doi.org/10.1016/j.jorganchem.2019.03.014.

References

[1] K.K.W. Lo, A.W.T. Choi, W.H.T. Law, Dalton Trans. 41 (2012) 6021–6047.
[2] D.L. Ma, H.Z. He, K.H. Leung, D.S.H. Chan, C.-H. Leung, Angew. Chem. Int. Ed. 52 (2013) 7666–7682.
[3] C.A. Puckett, R.J. Ernst, J.K. Barton, Dalton Trans. 39 (2010) 1159–1170.
[4] K.L. Haas, K.J. Franz, Chem. Rev 109 (2009) 4921–4960.
[5] E. Meggers, Chem. Commun. (2009) 1001–1010.
[6] (a) R.N. Dominey, B. Hauser, J. Hubbard, J. Dunham, Inorg. Chem. 30 (1991) 4754–4758;
(b) L. Sacksteder, M. Lee, J.N. Demas, B.A. DeGraff, J. Am. Chem. Soc. 115 (1993) 8230–8238;
(c) A.K. Pal, G.S. Hanan, Dalton Trans. 43 (2014) 11811–11814.
[7] (a) W.K. Smothers, M.S. Wrighton, J. Am. Chem. Soc. 105 (1983) 1067–1069;
(b) Y.S. Wang, S.X. Liu, M.R. Pinto, D.M. Dattelbaum, J.R. Schoonover, K.S. Schanze, J. Phys. Chem. A 105 (2001) 11118–11127.
[8] Y.L. Tung, P.C. Wu, C.S. Liu, Y. Chi, J.K. Yu, Y.H. Hu, P.T. Chou, S.M. Peng, G.H. Lee, Y. Tao, A.J. Carty, C.F. Shu, F.I. Wu, Organometallics 23 (2004) 3745–3748.
[9] K. Shinozaki, N. Takahashi, Inorg. Chem. 35 (1996) 3917–3924.
[10] S. Lamansky, P. Djurovich, D. Murphy, F. Abdel-Razzaq, H.E. Lee, C. Adachi, P.E. Burrows, S.R. Forrest, M.E. Thompson, J. Am. Chem. Soc. 123 (2001) 4304–4312.
[11] (a) K.K.W. Lo, M.-W. Louie, K.Y. Zhang, Coord. Chem. Rev. 254 (2010) 2603;
(b) V.W.W. Yam, K.M.C. Wong, Chem. Commun. 47 (2011) 11579;
(c) C.C. Ko, A.W.Y. Cheung, L.T.L. Lo, J.W.K. Siu, C.O. Ng, S.M. Yiu, Coord. Chem. Rev. 256 (2012) 1546;
(d) M. Panigati, M. Mauro, D. Donghi, P. Mercandelli, P. Mussini, L. de Cola, G. D'Alfonso, Coord. Chem. Rev. 256 (2012) 1621.
[12] (a) M.K. Kuimova, W.Z. Alsindi, J. Dyer, D.C. Grills, O.S. Jina, P. Matousek, A.W. Parker, P. Portius, X.Z. Sun, M. Towrie, C. Wilson, J. Yang, M.W. George, Dalton Trans. (2003) 3996;
(b) H. van der Salm, M.G. Fraser, R. Horvath, S.A. Cameron, J.E. Barnsley, X.Z. Sun, M.W. George, K.C. Gordon, Inorg. Chem. 53 (2014) 3126;
(c) H.-J. Nie, X. Chen, C.-J. Yao, Y.-W. Zhong, G.R. Hutchison, J. Yao, Chem. Eur J. 18 (2012) 14497;
(d) T. Yu, D.P.-K. Tsang, V.K.M. Au, W.H. Lam, M.-Y. Chan, V.W.-W. Yam, Chem. Eur J. 19 (2013) 13418;
(e) R. Horvath, M.G. Fraser, S.A. Cameron, A.G. Blackman, P. Wagner, D.L. Officer, K.C. Gordon, Inorg. Chem. 52 (2013) 1304.
[13] A.P. Zipp, Coord. Chem. Rev. 84 (1988) 47–83.
[14] V. Balzani, F. Scandola, Supramolecular Photochemistry, Ellis Horwood, Chichester, 1991.
[15] J.V. Caspar, B.P. Sullivan, T.J. Meyer, Organometallics 5 (1986) 1500–1502.
[16] (a) C.R. Carbera, H.D.J. Abruna, Elctroanal. Chem. Interfacial Electrochem. 209 (1986) 101–107;
(b) H. Takeda, K. Koike, T. Morimoto, H. Inumaru, O. Ishitani, Adv. Inorg. Chem. 63 (2011) 137–186.
[17] (a) T.A. Oriskovich, P.S. White, H.H. Thorp, Inorg. Chem. 34 (1995) 1629–1631;
(b) W.B. Connick, A.J.D. Bilio, M.G. Hill, J.R. Winkler, H.B. Gray, Inorg. Chim. Acta 240 (1995) 169–173.
[18] S. Bhattacharyya, M. Dixit, Dalton Trans. 40 (2011) 6112–6128.
[19] C. Sundararajan, T.R. Besanger, R. Labiris, K.J. Guenther, T. Strack, R. Garafalo, T.T. Kawabata, D. Finco-Kent, J. Zubieta, J.W. Babich, J.F. Valliant, J. Med. Chem. 53 (2010) 2612–2621.
[20] A.P. de Silva, D.B. Fox, A.J.M. Huxley, N.D. McClenagan, J. Roiron, Coord. Chem. Rev. 185–186 (1999) 297–306.
[21] J.P. Desvergne, A.W. Czarnik, Chemosensors of Ions and Molecules. NATO ASIC Series, Kluwer, Dordrecht, 1997.
[22] J.N. Demas, B.A. DeGraff, Anal. Chem. 63 (1991) 829A–837A.
[23] J.N. Demas, B.A. DeGraff, Coord. Chem. Rev. 211 (2001) 317–351.
[24] (a) E. Ioachim, E.A. Medlycott, G.S. Hanan, Inorg. Chim. Acta 359 (2006) 2599;
(b) M.-P. Santoni, E.A. Medlycott, G.S. Hanan, B. Hasenknopf, A. Proust, F. Nastasi, S. Campagna, C. Chiorboli, R. Agrazzi, F. Scandola, Dalton Trans. (2009) 3964.
[25] (a) D.J. Stufkens, A. Vlček Jr., Coord. Chem. Rev. 177 (1998) 127;
(b) A.K. Pal, G.S. Hanan, Chem. Soc. Rev. 43 (2014) 6184;
(c) A.K. Pal, P.K. Mandali, D.K. Chand, G.S. Hanan, Synlett 26 (2015) 1408.
[26] V. Balzani, A. Juris, Coord. Chem. Rev. 211 (2001) 97.
[27] S.P. Parua, D. Sinha, K.K. Rajak, Chem.Select. 3 (2018) 1120–1128.
[28] R. Sarkar, P. Mondal, K.K. Rajak, Dalton Trans. 43 (2014) 2859.
[29] P. Mondal, A. Hens, S. Basak, K.K. Rajak, Dalton Trans. 42 (2013) 1536.

[30] R. A. Agarwal S. Mukherjee, Polyhedron 106 (2016) 163–170.
[31] S.S. Kaye, J.R. Long, J. Am. Chem. Soc. 127 (2005) 6506.
[32] B. Valuer, Molecular Fluorescence: Principle and Applications, Wiley-BCH, Weinbeim, 2001.
[33] J. van Houten, R.J. Watts, J. Am. Chem. Soc. 98 (1976) 4853–4858.
[34] (a) A.D. Becke, J. Chem. Phys. 98 (1993) 5648–5652;
(b) C. Lee, W. Yang, R.G. Parr, Phys. Rev. B Condens. Matter 37 (1988) 785–789.
[35] (a) M.E. Casida, C. Jamoroski, K.C. Casida, D.R. Salahub, J. Chem. Phys. 108 (1998) 4439–4449;
(b) R.E. Stratmann, G.E. Scuseria, M.J. Frisch, J. Chem. Phys. 109 (1998) 8218–8224;
(c) R. Bauernschmitt, R. Ahlrichs, Chem. Phys. Lett. 256 (1996) 454–464.
[36] (a) V. Barone, M. Cossi, J. Phys. Chem. A 102 (1998) 1995–2001;
(b) M. Cossi, V. Barone, J. Chem. Phys. 115 (2001) 4708–4717;
(c) M. Cossi, N. Rega, G. Scalmani, V. Barone, J. Comput. Chem. 24 (2003) 669–681.
[37] (a) P.J. Hay, W.R. Wadt, J. Chem. Phys. 82 (1985) 270–283;
(b) P.J. Hay, W.R. Wadt, J. Chem. Phys. 82 (1985) 299–310.
[38] M.J. Frisch, G.W. Trucks, H.B. Schlegel, G.E. Scuseria, M.A. Robb, J.R. Cheeseman, G. Scalmani, V. Barone, B. Mennucci, G.A. Petersson, H. Nakatsuji, M. Caricato, X. Li, H.P. Hratchian, A.F. Izmaylov, J. Bloino, G. Zheng, J.L. Sonnenberg, M. Hada, M. Ehara, K. Toyota, R. Fukuda, J. Hasegawa, M. Ishida, T. Nakajima, Y. Honda, O. Kitao, H. Nakai, T. Vreven, J.A. Montgomery Jr., J.E. Peralta, F. Ogliaro, M. Bearpark, J.J. Heyd, E. Brothers, K.N. Kudin, V.N. Staroverov, R. Kobayashi, J. Normand, K. Raghavachari, A. Rendell, J.C. Burant, S.S. Iyengar, J. Tomasi, M. Cossi, N. Rega, J.M. Millam, M. Klene, J.E. Knox, J.B. Cross, V. Bakken, C. Adamo, J. Jaramillo, R. Gomperts, R.E. Stratmann, O. Yazyev, A.J. Austin, R. Cammi, C. Pomelli, J.W. Ochterski, R.L. Martin, K. Morokuma, V.G. Zakrzewski, G.A. Voth, P. Salvador, J.J. Dannenberg, S. Dapprich, A.D. Daniels, Ö. Farkas, J.B. Foresman, J.V. Ortiz, J. Cioslowski, D.J. Fox, GAUSSIAN 09 (Revision A.1), Gaussian, Inc., Wallingford, CT, 2009.
[39] N.M. O'Boyle, A.L. Tenderholt, K.M. Langner, J. Comput. Chem. 29 (2008) 839–845.
[40] G.M. Sheldrick, Acta crystallogr, Sect. A: Found. Crystallogr. 64 (2008) 112.
[41] G.M. Sheldrick, SHELEXL 97 (1997).